Supporting Information for

Solvent-induced conformational changes in cyclic peptides: A vibrational circular dichroism study

Christian Merten[a,b], Fee Li[b], Kenny Bravo-Rodriguez[c], Elsa Sanchez-Garcia[c], Yunjie Xu[a], Wolfram Sander[b]

[a] University of Alberta, Department of Chemistry, Edmonton, Alberta, T6G2G2, Canada

[b] Ruhr-Universität Bochum, Fakultät für Chemie und Biochemie, 44801 Bochum, Germany

[c] Max-Planck-Institut für Kohlenforschung, 45470 Mülheim an der Ruhr, Germany

Content:

1.	Comparison of experimental spectra	p. 2
2.	Example structures obtained from the conformational analysis	p. 3
3.	Conformational analysis	p. 6
4.	Single conformer spectra	p. 7
5.	Raman spectra of **1** and ***D*-2**	p. 10
6.	Calculated spectra and conformation of explicitly solvated **1**	p. 11
7.	Replica Exchange Molecular Dynamics Simulations of **1**	p. 12

1. Comparison of experimental spectra

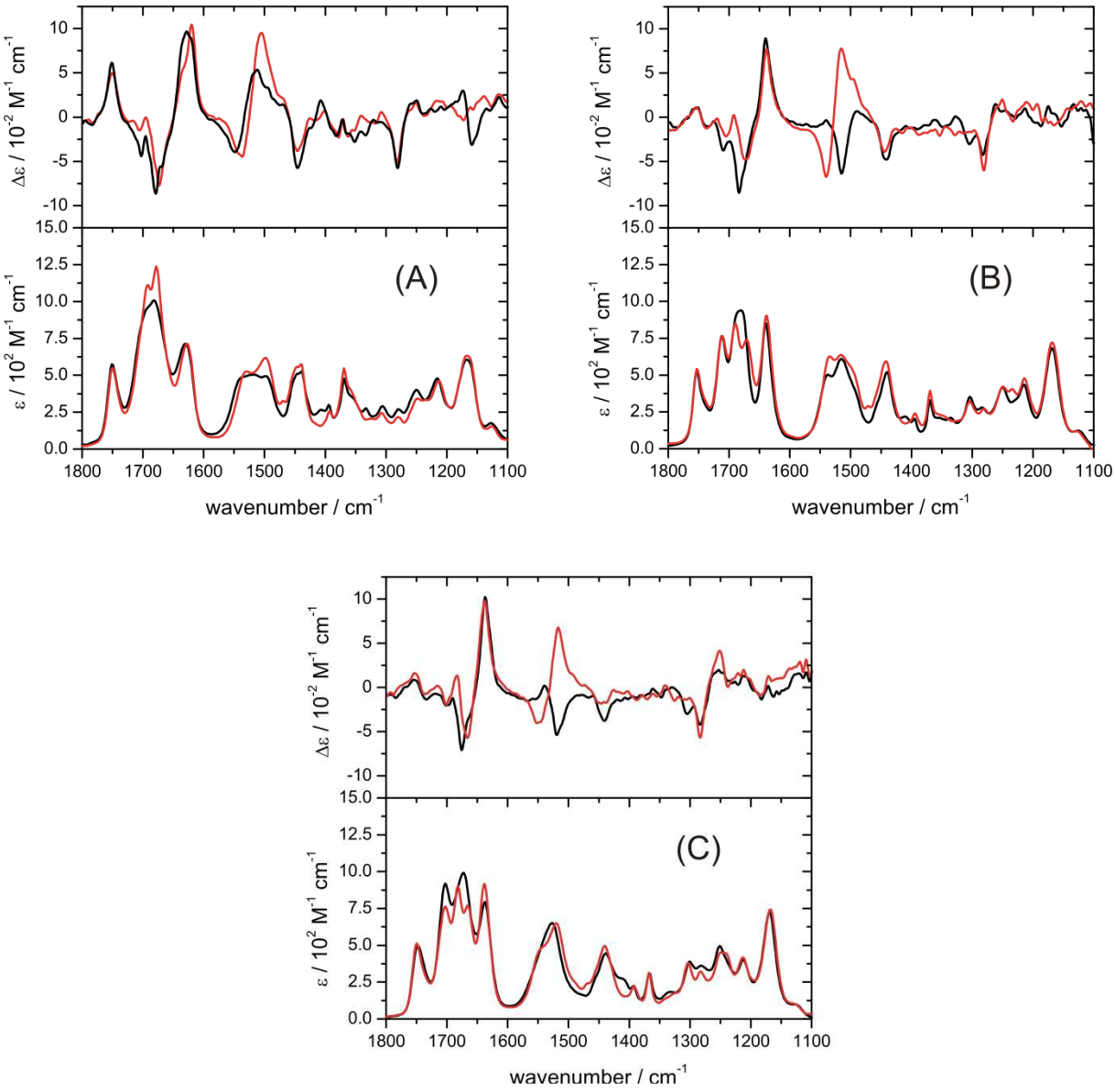

Fig. S1. Direct comparison of the experimental IR and VCD spectra of **1** (black) and ***D*-2** (red) in chloroform-d_1 (A), acetonitrile-d_3 (B), and dimethyl sulfoxide-d_6 (C).

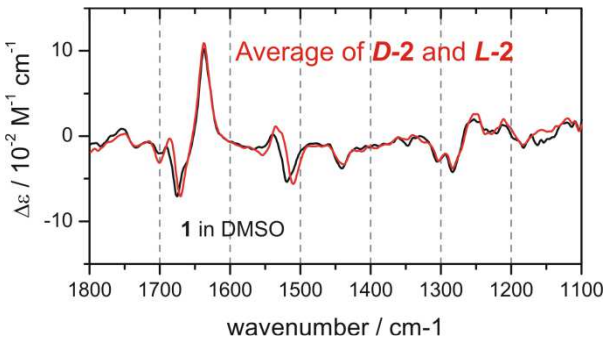

Fig. S2 Comparison of the experimental VCD spectrum of **1** in DMSO with the calculated average of the VCD spectra of ***D*-** and ***L*-2** in DMSO.

2. Example structures obtained from the conformational analysis

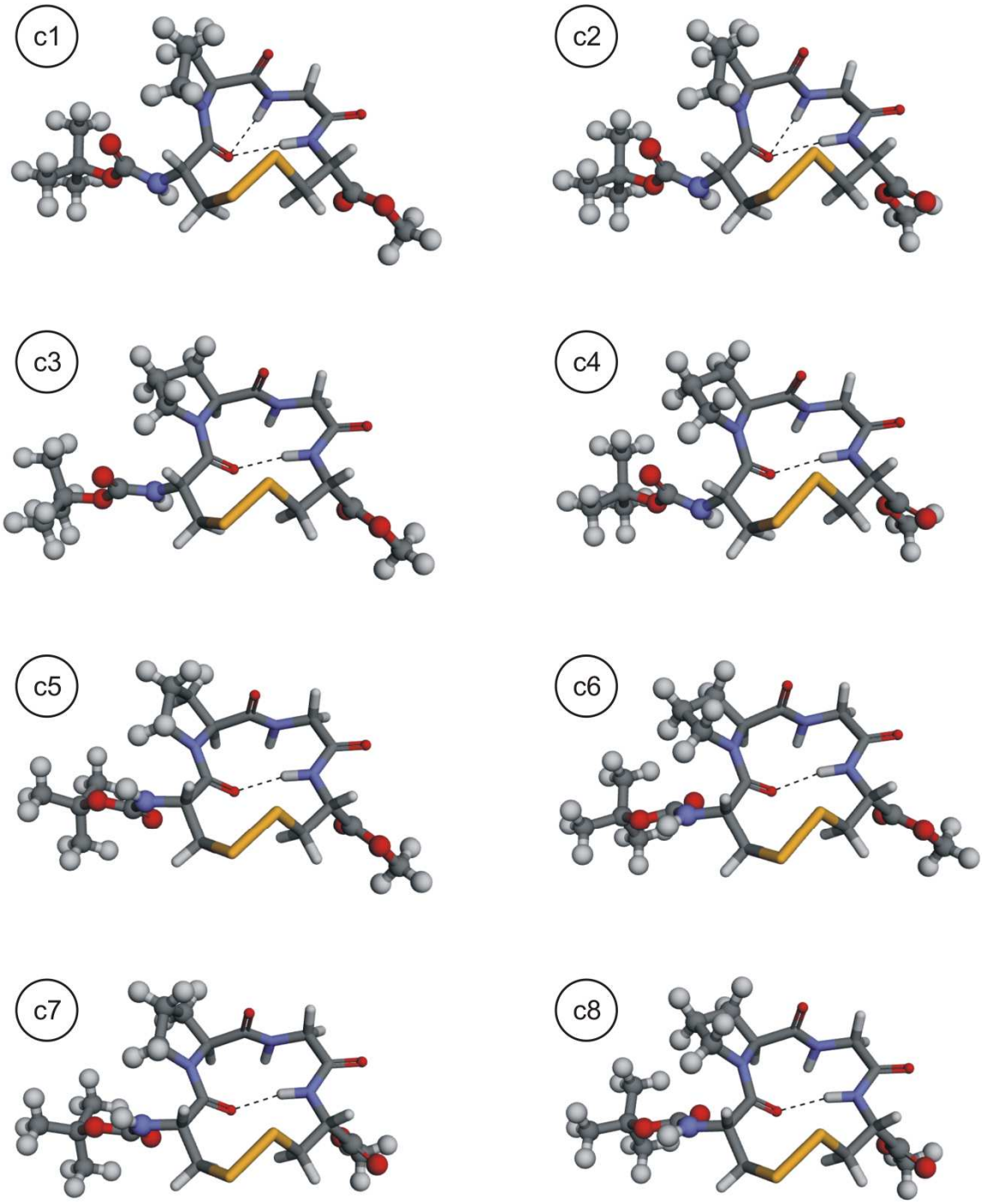

Fig. S3. The eight evaluated side-group conformations c1-c8 exemplified for the ring-structure r1 optimized in gas phase.

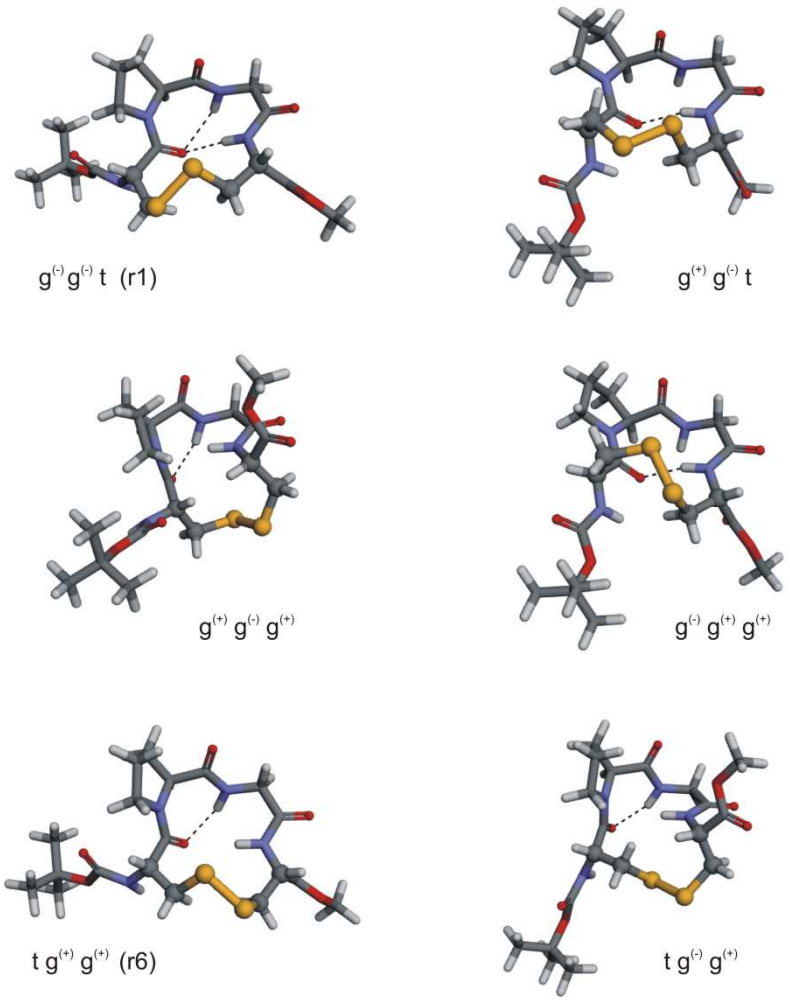

Fig. S4. Structure of the six disulfide bridge conformers considered for VCD spectra calculations.

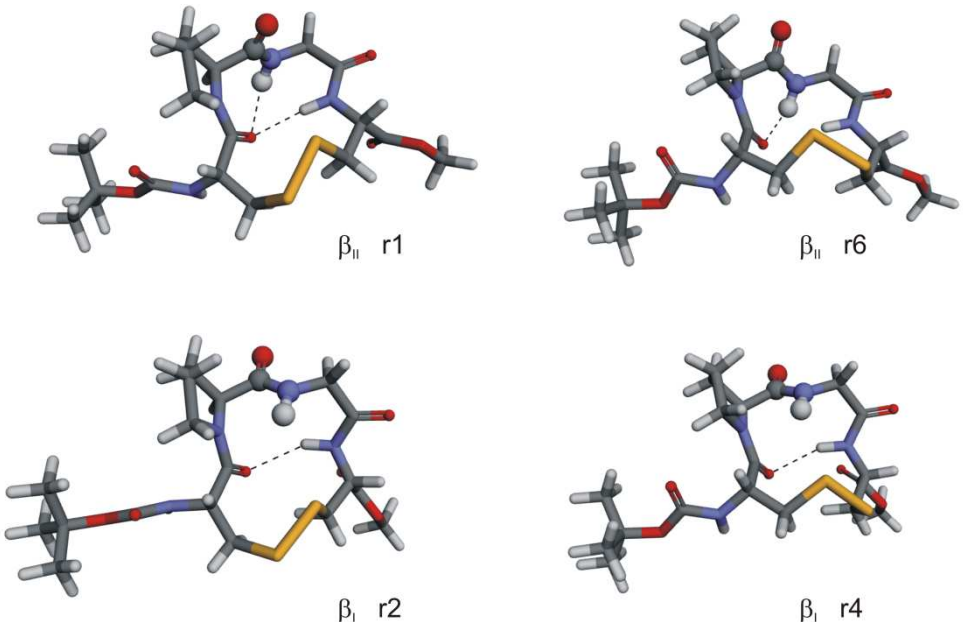

Fig. S5 The β_{II} ring structures r1 and r6 compared to the corresponding β_{I} structure r2 and r4

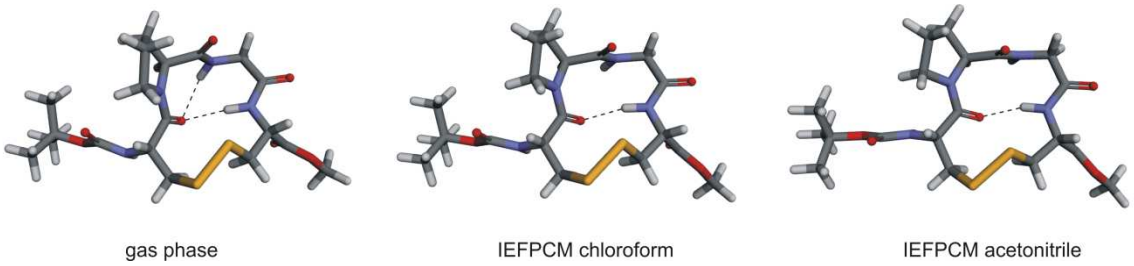

Fig. S6 The β_{II} ring structure r1 optimized in gas phase and using the IEFPCM.

3. Conformational analysis

Table S1. Relative energies and corresponding Boltzmann populations for all calculated conformers. Energies are referenced to the lowest energy structure of the respective set of calculations.

	Relative energy differences in kcal/mol						Boltzmann populations (in %)					
	gas phase		chloroform		acetonitrile		gas phase		chloroform		acetonitrile	
	DE	DG	DE	DG	DE	DG	DE	DG	DE	DG	DE	DG
r1-c1	0.0	0.0	0.7	1.1	1.0	1.3	8.8	12.3	3.3	3.3	4.6	5.7
r1-c2	0.7	0.6	1.5	1.8	1.5	1.8	2.7	4.4	0.8	1.1	1.9	2.3
r1-c3	0.7	0.8	0.5	1.3	0.9	1.8	2.7	3.4	4.7	2.1	5.5	2.4
r1-c4	2.4	2.3	1.6	2.4	1.8	2.0	0.2	0.3	0.6	0.4	1.2	1.5
r1-c5	1.4	1.3	1.1	2.0	1.5	2.5	0.8	1.4	1.6	0.7	2.1	0.6
r1-c6	3.0	2.5	2.2	2.7	2.0	1.7	0.1	0.2	0.2	0.2	0.8	2.9
r1-c7	4.4	4.8	3.5	4.3	3.6	4.5	0.0	0.0	0.0	0.0	0.1	0.0
r1-c8	3.8	4.1	3.0	3.8	3.1	3.9	0.0	0.0	0.1	0.0	0.1	0.1
r2-c1	2.3	2.0	1.9	1.5	2.0	1.7	0.2	0.4	0.4	1.7	0.8	2.9
r2-c2	2.3	1.8	2.2	2.3	2.5	2.4	0.2	0.6	0.2	0.4	0.4	0.9
r2-c3	3.0	2.7	2.4	2.6	2.7	3.1	0.1	0.1	0.2	0.3	0.3	0.3
r2-c4	4.4	3.5	2.9	2.8	23.1	22.9	0.0	0.0	0.1	0.2	0.0	0.0
r2-c5	3.0	2.6	2.6	2.9	3.0	3.0	0.1	0.2	0.1	0.2	0.2	0.3
r2-c6	4.1	3.7	2.9	3.6	2.7	3.4	0.0	0.0	0.1	0.0	0.3	0.2
r2-c7	5.3	5.8	4.3	5.2	4.1	5.1	0.0	0.0	0.0	0.0	0.0	0.0
r2-c8	5.6	6.1	4.2	4.9	3.5	4.0	0.0	0.0	0.0	0.0	0.1	0.1
r4-c1	0.7	0.3	0.6	1.1	0.6	0.0	2.7	7.5	3.7	3.2	9.0	47.6
r4-c2	0.2	0.3	0.4	0.4	0.4	1.3	6.0	7.9	5.1	11.0	12.2	5.5
r4-c3	1.6	1.0	0.1	0.0	0.0	0.6	0.6	2.4	8.5	20.6	25.5	16.3
r4-c4	5.3	5.4	3.1	3.6	1.7	2.2	0.0	0.0	0.1	0.0	1.5	1.2
r4-c5	0.6	0.1	0.0	0.7	0.4	1.6	3.1	10.9	10.2	5.8	14.0	3.4
r6-c1	1.0	1.0	2.1	1.8	3.7	4.0	1.5	2.4	0.3	1.1	0.0	0.1
r6-c2	1.2	0.7	2.6	3.2	4.0	4.4	1.1	4.0	0.1	0.1	0.0	0.0
r6-c3	2.0	1.5	2.3	2.3	3.0	3.2	0.3	1.0	0.2	0.4	0.2	0.2
r6-c4	4.6	4.2	4.5	5.2	4.9	5.4	0.0	0.0	0.0	0.0	0.0	0.0
r6-c5	2.7	2.1	3.0	4.7	3.5	3.8	0.1	0.4	0.1	0.0	0.1	0.1
r6-c6	5.7	5.7	5.1	5.8	5.3	5.5	0.0	0.0	0.0	0.0	0.0	0.0
r6-c7	6.7	6.4	5.8	6.9	5.7	6.6	0.0	0.0	0.0	0.0	0.0	0.0
r6-c8	5.7	5.4	5.0	5.4	5.3	6.1	0.0	0.0	0.0	0.0	0.0	0.0
r7-c1	-1.0	-0.3	-0.9	-0.1	0.2	1.2	47.6	20.3	42.8	23.3	18.8	6.1
r7-c2	-0.5	-0.2	-0.3	-0.1			18.8	17.7	16.9	23.7		
r22-c1	0.9	1.0					2.0	2.1				
r16-c1	2.1	3.0					0.3	0.1				
r3-c1	1.9	2.6	2.7	4.2			0.4	0.1	0.1	0.0		

4. Single-conformer spectra

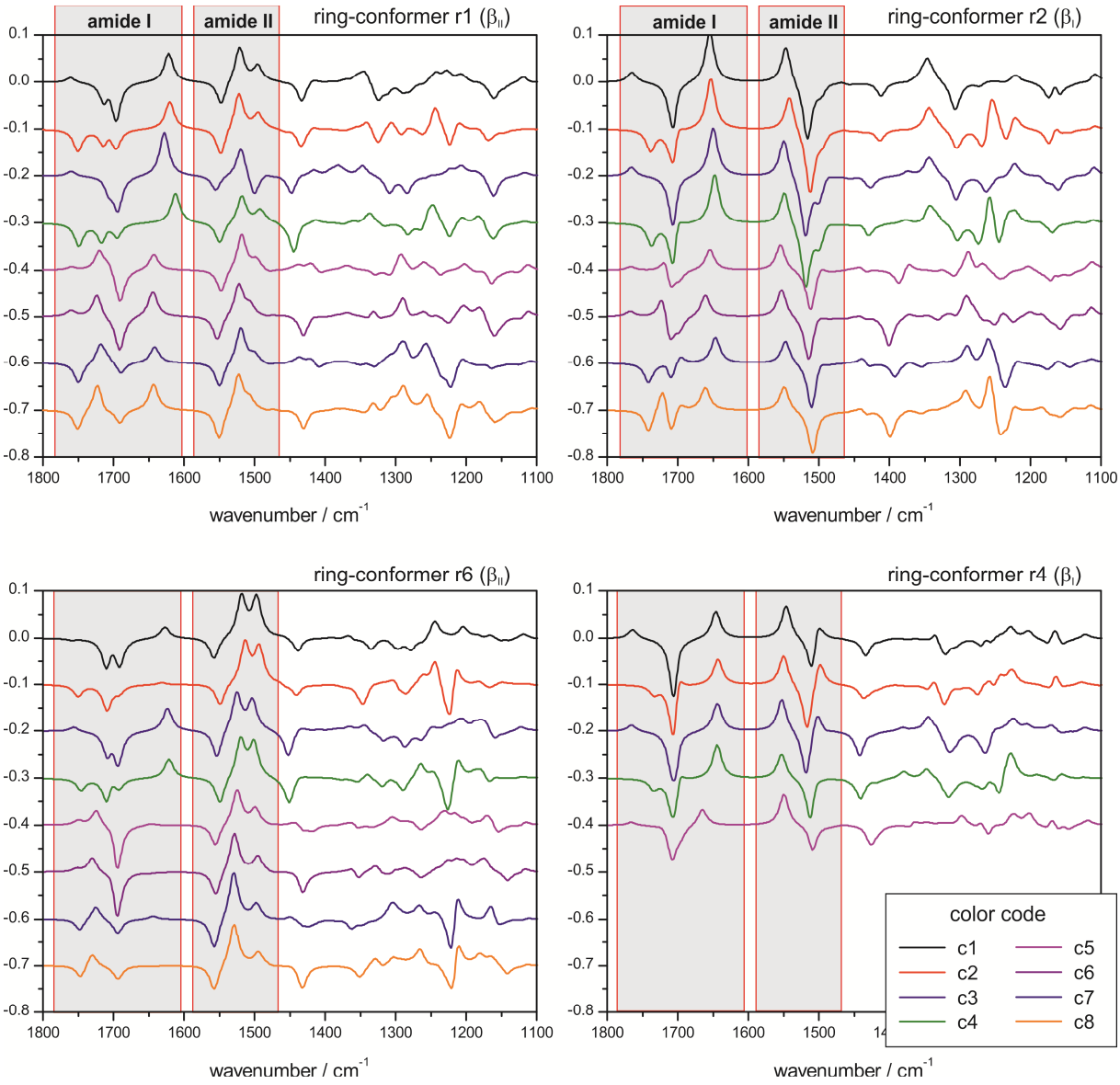

Fig. S6. Calculated gas phase VCD spectra for the eight side-group conformations c1-c8 of the β_{II}-type ring structures r1 and r6 ($g^{(-)}g^{(-)}t$ and $tg^{(+)}g^{(+)}$, respectively) and their corresponding β_I structures r2 and r4. Since the trend was obvious, the higher energy conformers of r4 were not calculated.

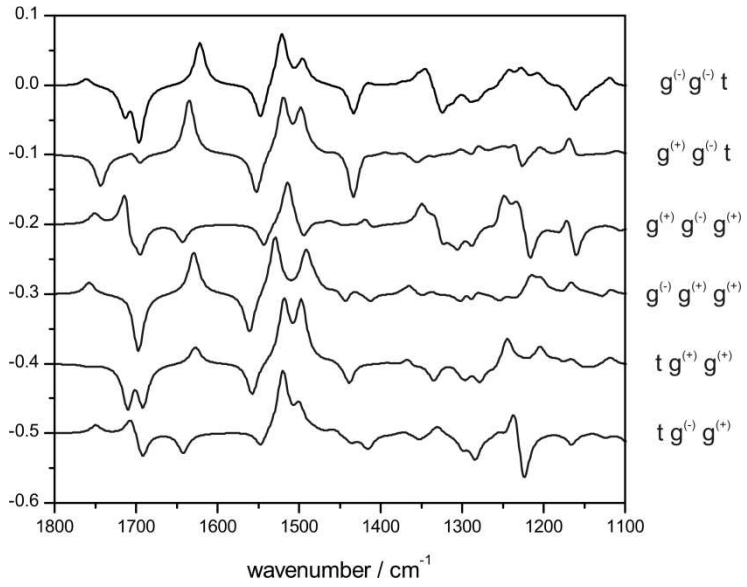

Fig. S7. Calculated gas phase VCD spectra for different disulfide bridge conformations with β_{II}-turn structure and side-group conformation c1 (see structures below).

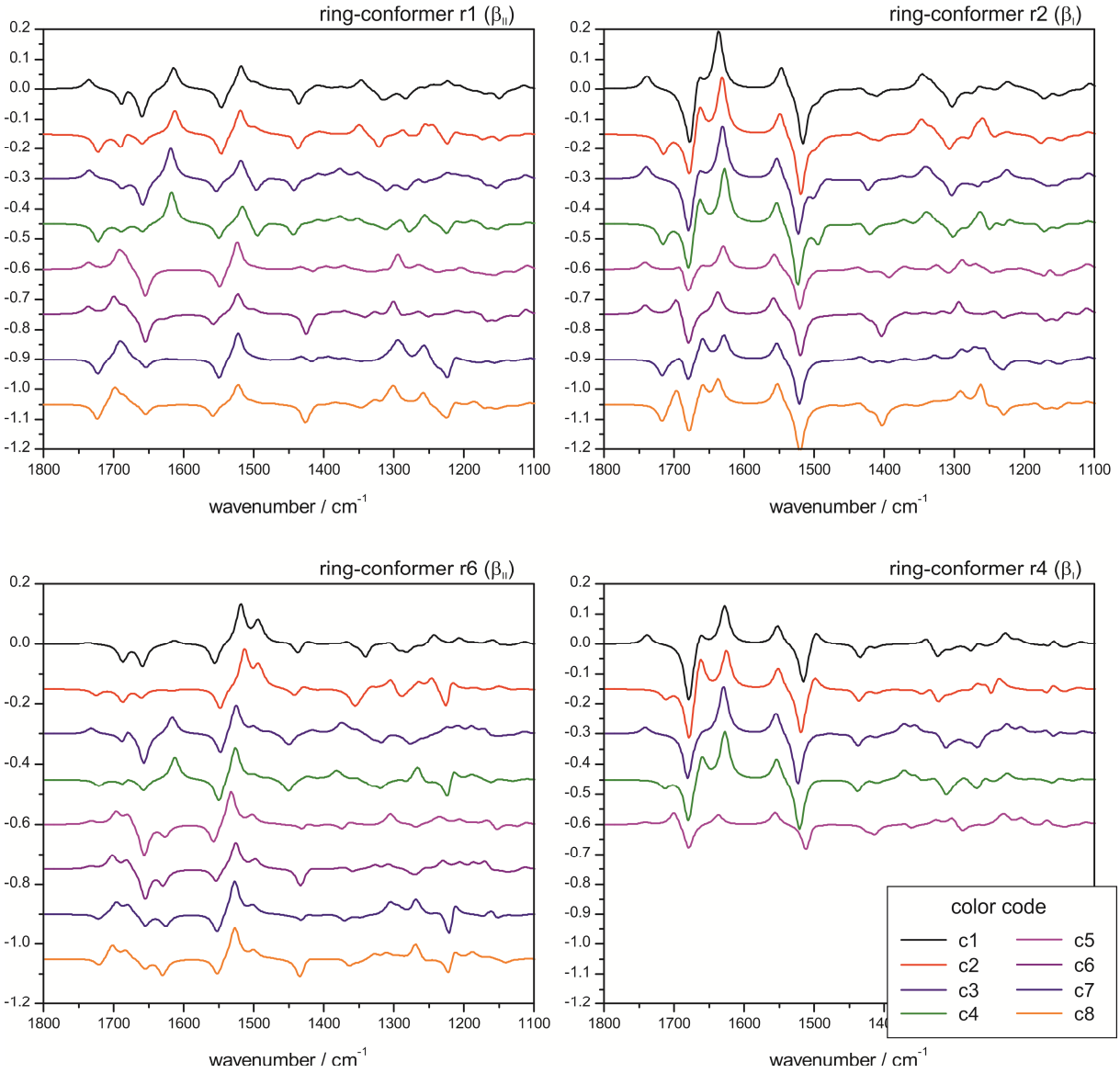

Fig. S8. Calculated VCD spectra (IEFPCM chloroform) for the eight side-group conformations c1-c8 of the β_{II}-type ring structures r1 and r6 ($g^{(-)}g^{(-)}t$ and $tg^{(+)}g^{(+)}$, respectively) and their corresponding β_I structures r2 and r4.

5. Raman spectra of 1 and *D*-2

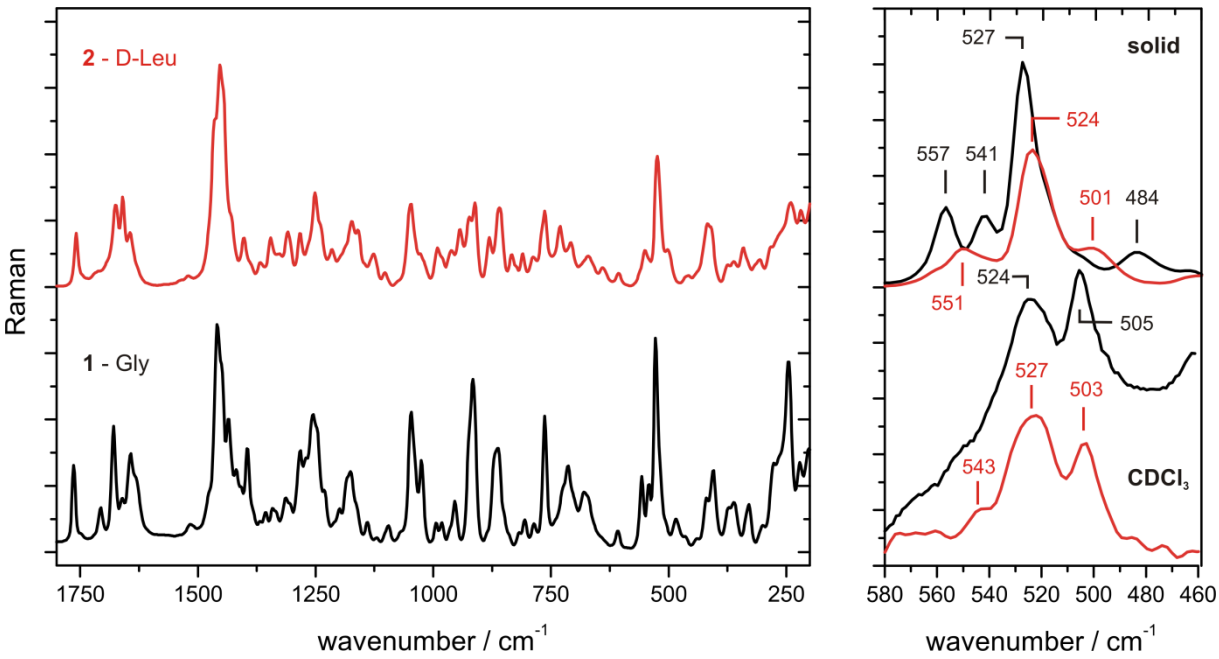

Fig.S9 Raman spectra of **1** and ***D*-2** in solid state (left) and in saturated $CDCl_3$ solution (~100 mg/ml)

Raman spectroscopy is very sensitive to the conformation of the disulfide bridge. In order to probe the conformational freedom of the disulfide bridges in **1** and ***D*-2**, Raman spectra were measured in solid state and for a saturated solution of the peptides in $CDCl_3$ on a Bruker IFS 66/S spectrometer equipped with an FRA 106/S Raman module at an excitation wavelength of 1064 nm and a collection time of 30 min. Due to the low amount of material left for these supporting measurements, only a small amount of solution was prepared and filled into a melting point capillary. The solubility in acetonitrile or DMSO was too low to obtain publishable spectral data. However, in the DMSO spectrum of **1** a broad and weak band with a maximum around 515 cm^{-1} was observed.

The conformation of disulfide bridges are typically described by the three torsional angles of the C^{α}-C-S-S-C-C^{α} unit as gauche-gauche-gauche (ggg), trans-gauche-gauche (tgg or ggt), and trans-gauche-trans (tgt). These three conformations give to rise to slightly different band positions for the S-S stretching vibration in Raman spectra, namely at 510 cm^{-1} for the ggg-isomer, at 525 cm^{-1} for the ggt isomer, and at 540 cm^{-1} for the tgt isomer.[1] In the right panel of Figure S9, it can clearly be seen that both peptides adopt a ggt conformation in solid state as it is found for the crystal structure. However, in chloroform solution, both peptides feature a clear Raman band at ~505 cm^{-1} which indicates the presence of conformers in the ggg-conformation.

[1] A. T. Tu, *Journal of the Chinese Chemical Society* **50** (2003) 1-10

6. Calculated spectra and conformation of explicitly solvated 1

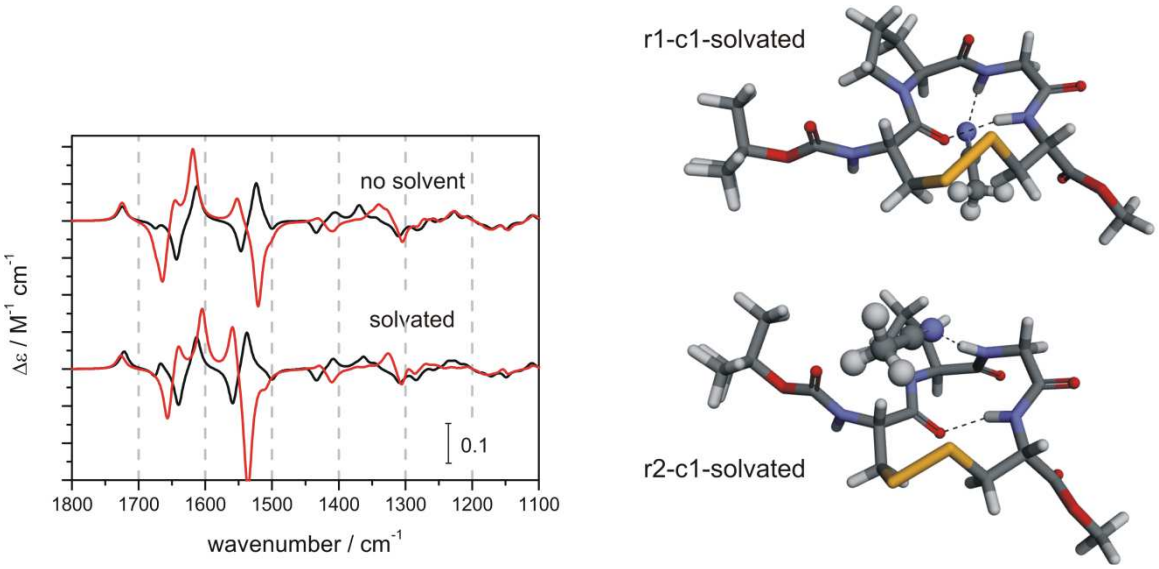

Fig. S10 Comparison of the calculated VCD spectra of r1-c1 and r2-c1 with and without explicit solvation.

7. Replica Exchange Molecular Dynamics Simulations of 1

Both β turns feature Cys(1)-CO···Cys(4)-NH interactions and can in general form Gly-NH-acetonitrile hydrogen bonds. In the case of the β_{II} structures, the formation of the Gly-NH-acetonitrile hydrogen bond is competing with the formation of an intramolecular hydrogen bond between Gly-NH and Cys(1)-CO. Accordingly, the structural analysis indicates that for the most populated states a Cys(1)-CO···Gly-NH hydrogen bond can be found in addition to the Cys(1)-CO···Cys(4)-NH interaction (Table S2). This, however, leads to a competition between Cys(4)-NH and Gly-NH for the carbonyl group of Cys(1) which is reflected in the somehow larger Cys(1)···Cys(4)-NH average hydrogen bond distance (2.9 ± 0.6 Å) in acetonitrile with respect to the value in the crystal structure (2.4 Å). There, the interactions with Pro and Gly play a much less relevant role (Cys(1)-CO···Gly-NH: 3.3 Å and Pro-CO···Cys(4)-NH: 3.1 Å). Although the Pro-CO···Cys(4)-NH interaction may theoretically help to stabilize the β_I structures in solution, the averaged hydrogen bond distances and conformer populations suggest that this interaction is less relevant than the Cys(1)-CO ···Cys(4)-NH and Cys(1)-CO···Gly-NH interactions (Table S2) .

Thus, the formation of hydrogen bonds between Cys(1)-CO···Gly-NH could be an important factor determining the preference of the β_{II} motif over the β_I structure. On the other hand, the Gly-NH group can also be engaged in interactions with the solvent. Intuitively, the Cys(1)-CO···Gly-NH hydrogen bond is expected to be more relevant in solvents with less H acceptor capability, or, in other words, in solvents which have less tendency to interact with Gly-NH. Accordingly, we expect that in better hydrogen acceptor solvents such as acetonitrile or DMSO, Gly-NH-solvent interactions would be more favoured than predicted by the MD simulations thus contributing to increase the population of β_I conformers.

Table S2. Cys(1)-CO···Gly-NH, Pro-CO··Cys(4)-NH, and Cys(1)-CO···Cys(4)-NH hydrogen bond distances distribution for the trajectory at 300 K of the REMD simulation. Distance ranges are A: d ≤ 2.2, B: 2.2 < d ≤ 3.0, C: 3.0 < d ≤ 4.0 and D: d > 4.0. All distances are given in Å.

Total REMD					β-I					β-II				
Cys(1)-CO···Gly-NH														
Range	A	B	C	D	Range	A	B	C	D	Range	A	B	C	D
	12	52	34	2		0	10	71	19		11	57	32	0
Average	2.8 ± 0.5				Average	3.6 ± 0.5				Average	2.8 ± 0.4			
Pro-CO···Cys(4)-NH														
Range	A	B	C	D	Range	A	B	C	D	Range	A	B	C	D
	4	65	27	4		4	40	45	11		4	69	25	2
Average	2.9 ± 0.6				Average	3.2 ± 0.8				Average	2.8 ± 0.5			
Cys(1)-CO···Cys(4)-NH														
Range	A	B	C	D	Range	A	B	C	D	Range	A	B	C	D
	0	18	77	5		0	3	76	22		0	20	78	2
Average	3.4 ± 0.4				Average	3.8 ± 0.4				Average	3.3 ± 0.4			

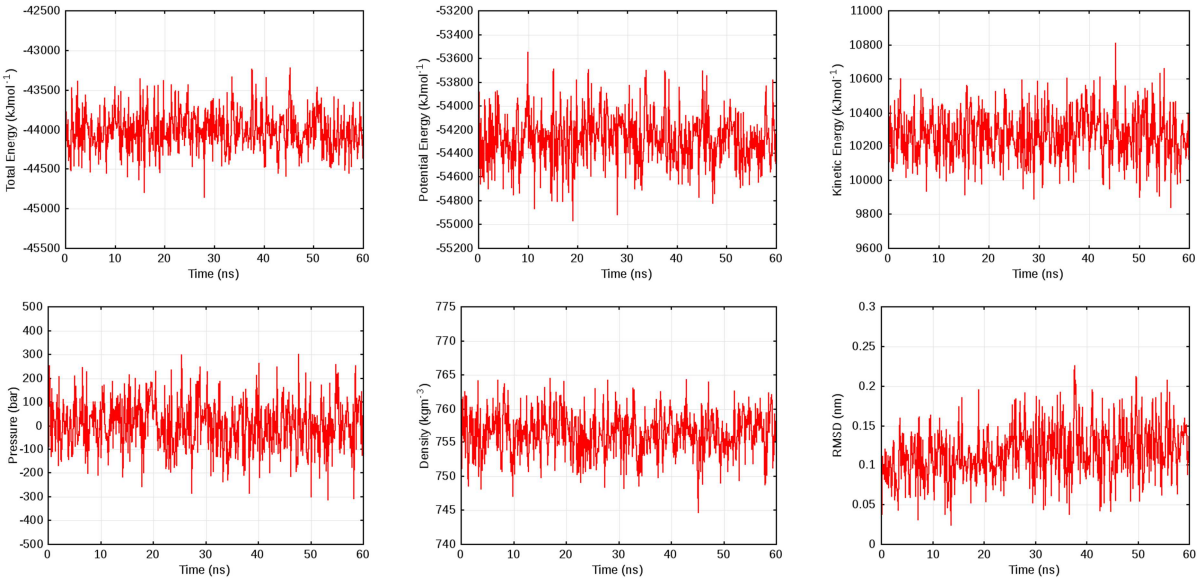

Fig. S11. Time evolution of total, potential and kinetic energies, pressure, density and RMSD for the REMD simulation at 300 K.

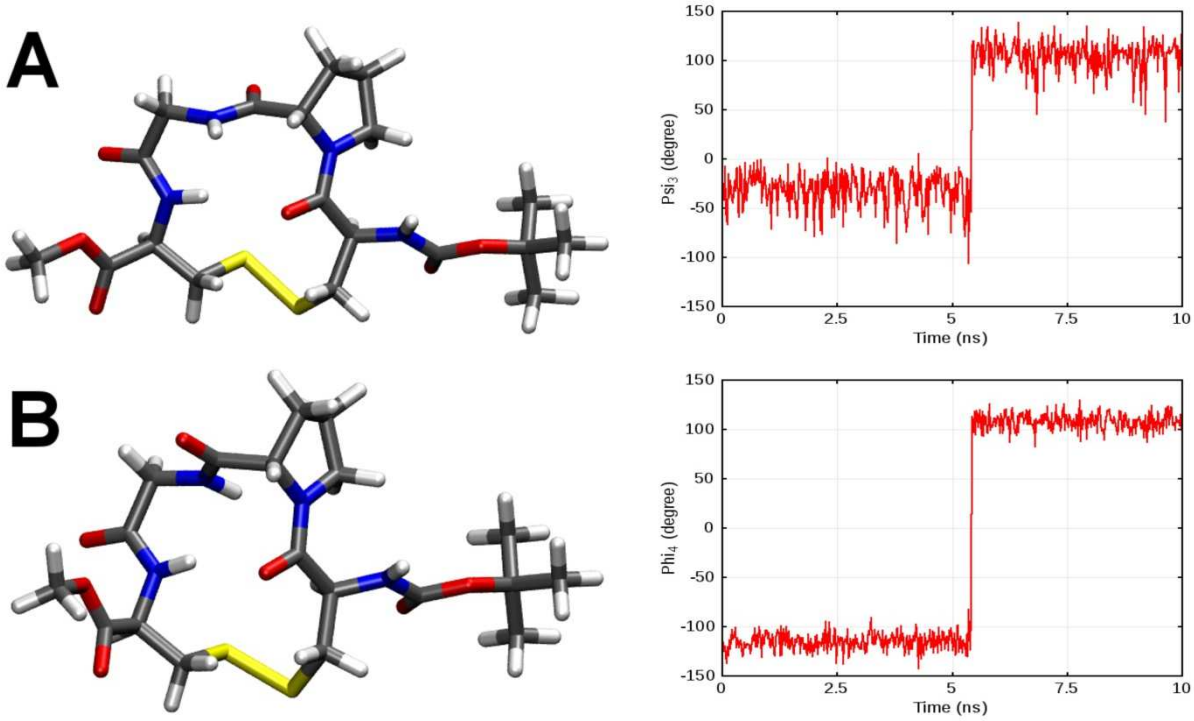

Fig. S12. Time evolution of Ψ_{Pro} and Φ_{Gly} during the 10 ns NPT simulation of **1** at 290 K starting from a β_I motif (B) which converts to a β_{II} structure (A)

Replica exchange statistics

Repl 20964 attempts, 10482 odd, 10482 even

Repl average probabilities:

Repl	0	1	2	3	4	5	6	7	8	9	10	11	12	13	14	15	16	17	18	19	20	21	22	23	24	25	26	27	28	29	30	31	32
Repl	.39	.50	.46	.46	.42	.48	.46	.55	.47	.43	.47	.44	.50	.45	.48	.46	.51	.48	.48	.51	.45	.48	.44	.49	.54	.46	.48	.47	.48	.50	.42	.51	

Repl number of exchanges:

Repl	0	1	2	3	4	5	6	7	8	9	10	11	12	13	14	15	16	17	18	19	20	21	22	23	24	25	26	27	28	29	30	31	32
Repl	4032	5250	4801	4780	4403	4971	4896	5700	4971	4537	4903	4629	5275	4703	4996	4831	5363	4995	5026	5294	4704	5080	4581	5129	5674	4841	5032	4880	5008	5251	4480	5397	

Repl average number of exchanges:

Repl	0	1	2	3	4	5	6	7	8	9	10	11	12	13	14	15	16	17	18	19	20	21	22	23	24	25	26	27	28	29	30	31	32
Repl	.38	.50	.46	.46	.42	.47	.47	.54	.47	.43	.47	.44	.50	.45	.48	.46	.51	.48	.48	.51	.45	.48	.44	.49	.54	.46	.48	.47	.48	.50	.43	.51	